

Single Phosphorus Ion Implantation into Prefabricated Nanometre Cells of Silicon Devices for Quantum Bit Fabrication

Changyi YANG, David N. JAMIESON, Chris PAKES, Steven PRAWER, Andrew DZURAK¹, Fay STANLEY¹, Paul SPIZZIRI, Linda MACKS¹, Eric GAUJA¹ and Robert G. CLARK¹

Centre for Quantum Computer Technology, School of Physics, University of Melbourne, Victoria 3010, Australia

¹Centre for Quantum Computer Technology, University of New South Wales, Sydney 2052, Australia

(Received November 7, 2002; accepted for publication November 29, 2002)

In the near future, devices that employ single atoms to store or manipulate information will be constructed. For example, a solid-state quantum computer has been proposed that encodes information in the nuclear spin of shallow arrays of single ³¹P atoms (quantum bits or qubits) in a matrix of pure silicon. Construction of these devices presents formidable challenges. One strategy is to use single ion implantation, with the energy range of 10 to 20 keV, to load the qubits into prefabricated cells of the device with a period of a few tens of nanometres. We have developed a method of single ion implantation that employs detector electrodes adjacent to the prefabricated qubit cells that can detect on-line single keV ion strikes appropriate for the fabrication of shallow arrays. Our method of the sub-20 keV single ion detection utilizes a pure silicon substrate with a very high resistivity, a thin (5 nm) SiO₂ surface layer, biased electrodes applied to the surface and sensitive electronics that can detect the charge transient from single keV ion strikes. We show that our detectors have a near 100% efficiency for keV ions, extremely thin dead layer thickness (~5 nm) and a wide sensitive region extending laterally from the electrodes (greater than 15 μm) where the nanometre cells can be constructed. We compare the method with the other methods, such as those of measuring the secondary electrons or phonons induced by single ion impacts. [DOI: 10.1143/JJAP.42.4124]

KEYWORDS: qubit, single ion implantation, keV single ion detection

1. Introduction

In the Kane quantum computer scheme, an array of ³¹P atoms needs to be embedded in ²⁸Si substrate with nanometre accuracy.¹⁾ This scheme is promising for its scalability to large arrays and compatibility with existing silicon technology. Several construction methods are being developed. Precision lithography based on scanning tunneling microscope (STM) machining of a hydrogen terminated silicon surface followed by attachment of PH₃ from a gas ambient, removal of the hydrogen and overgrowth of a thin epilayer of silicon (10–20 nm) is one very promising possibility.²⁾ However, before this highly challenging possibility can be accomplished, the ion implantation method, using 10–20 keV ³¹P ions, offers a fast route to the fabrication of a device containing a few qubits.³⁾ It is highly desirable to rapidly fabricate a small number of qubits to test some of the crucial parameters of the silicon based quantum computer system, such as to test the control and read out of the qubit states and to measure the qubit decoherence time.

For the purpose of the single ion implantation and registration, successful ion detection can be achieved by detecting any physical signal resulting from the incident ion interaction with the substrate material to be implanted. Various physical processes occurring in the ion-solid interaction produce different types of signals that may be used as a means to detect a single ion arrival in the substrate. These include luminescence, secondary electrons, phonons and electron-hole (e-h) pairs. We compare these different methods and focus on the method of e-h pair detection and demonstrate how to incorporate this ion detection method in the nano-fabrication process for a practical device.

2. Methods of Low Energy Heavy Ion Detection

When a fast ion is incident into a semiconductor, the interaction of the ion with the matter produces a few types of signals simultaneously. In Fig. 1, the induced luminescence and secondary electrons (SE) are emitted from the substrate

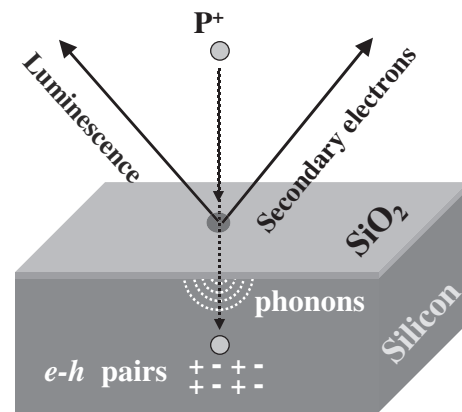


Fig. 1. Single-ion detection methods. The induced luminescence and secondary electrons are emitted from the substrate surface, whereas phonons and electron-hole pairs are generated in the vicinity of the ion track inside the substrate.

surface, whereas phonons and electron-hole pairs are generated in the vicinity of the ion track inside the substrate.

The ion-beam-induced-luminescence method can be easily applied for the detection of single high-energy ion implantation into phosphors.⁴⁾ However, clearly the luminescence method, based on the radiative recombination of the e-h pairs, is not very favorable for pure, single crystal, silicon material because the luminescence yield is very low owing to its indirect band gap. In addition, the luminescence must escape from the surface before reaching a luminescence detector and only about 1–10% of photons can escape from the surface due to large internal reflection loss.

Normally, one to a few secondary electrons are emitted from the surface upon each single ion strike. The number depends on the type of ion species and the surface condition. It is highly challenging to accomplish a simple detection method with 100% detection efficiency for a single secondary electron. However, the method of secondary electron detection has been successfully applied in a focused

ion beam (FIB) system for single ion implantation (SII) of semiconductor devices with a sub-100 nm feature size, for suppressing the donor fluctuation in small devices.⁵⁾ Up to 90% detection efficiency for single ion implantation has been achieved in such systems using an electron detector, which consists of a scintillator and a photomultiplier tube.⁶⁾ The secondary electron yield can be largely increased when highly charged ions are to be used, and close to 100% detection efficiency can be achieved. It was reported that a 9 keV P^{15+} ion striking a silicon substrate, produces about 20 secondary electrons from the surface.⁷⁾ However, the highly charged ion may cause a relatively large amount of damage in the substrate due to the “Coulomb explosion” effect. However the primary disadvantage of the method of detecting SE signals is the incompatibility with the use of a nanometer mask, which is essential to position the implantation site with nanometer accuracy if a beam of nanometer resolution is not available.

The energy dissipation of the incident ions in the substrate gives rise to phonon signals, which can be used for the detection of single ion arrival in the substrate. A sensitive thermal sensor, coupled to a very small volume (~ 10 microgram) silicon substrate, may detect 1 keV phonon energy by measuring the small temperature rise (~ 40 mK).⁸⁾ This requires the small volume substrate to be maintained at sub-100 mK temperature.⁸⁾ The major difficulty is the requirement to handle the very small mass volume (small heat capacity) of the substrate and to use a sub-100 mK cryogenic facility within the ion implantation system, making the method challenging to incorporate into a practical system.

Apart from the phonon production part of the process of the incident ion energy dissipation in the silicon substrate, the electronic stopping of the incident ion produces e-h pairs with a very long lifetime ($> 20 \mu s$) in a high-quality silicon substrate. Under the influence of built-in electric fields, produced by biasing two paired electrodes, the e-h carriers drift separately towards opposite electrodes, producing a charge pulse in a charge-sensitive-amplifier, coupled to one of the biased electrodes. The charge pulse provides rich information on the arrival of incident ions and potentially provides information on the ion stopping depth. We have proposed the use of this novel ion detection method to

construct a two-donor device and propose to develop the method further for the production of large donor arrays.

3. Electron-hole Pair Production and Charge Pulse Formation

When ions are incident into solid state matter, a part of the energy dissipates in the substrate through an electronic stopping process, which channels a part of the initial energy into the ionization energy to produce e-h pairs, and a nuclear stopping process, which results in the host atom recoiling with the production of phonons. Following each primary nuclear stopping event, if the energy of the recoiling atom and the residual energy of the scattered projectile are sufficiently high, a further dissipation of these energies may lead to a contribution in the e-h pair production by the subsequent slowing down of these particles in the matrix through an electronic-stopping process. The movement of the e-h pairs generated in the active volume of the substrate form a charge pulse signal in the charge-sensitive pre-amplifier coupled to one of the electrodes, with the pulse height proportional to the number of e-h pairs generated by the total ionization energy when the charge pulse is integrated over 1–10 μs . The energy loss through nuclear stopping processes does not contribute to the charge pulse formation; only the energy loss through the electronic stopping process gives rise to the charge pulse. The energy loss in the top dead-layer, normally a passivation layer, also does not contribute to the formation of a charge pulse.

Common radiation detectors are designed for ions with a few MeV/amu or for X-ray detection, where almost 100% of the incident energy converts to ionization energy and hence the production of e-h pairs. The number of e-h pairs produced is linearly proportional to the ionization energy in the substrate. However, for sub-20 keV heavy ions, required for the construction of shallow arrays, only a very small part of the initial incident energy contributes to the production of e-h pairs. This makes the charge pulse height significantly reduced compared to full conversion of the kinetic energy to e-h pairs. This is known as the pulse-height-defect (PHD).⁹⁾ The PHD mainly results from the energy loss through the nuclear stopping process.

Figure 2 compares the PHD values between different incident ions and X-rays. The data was recalculated partly

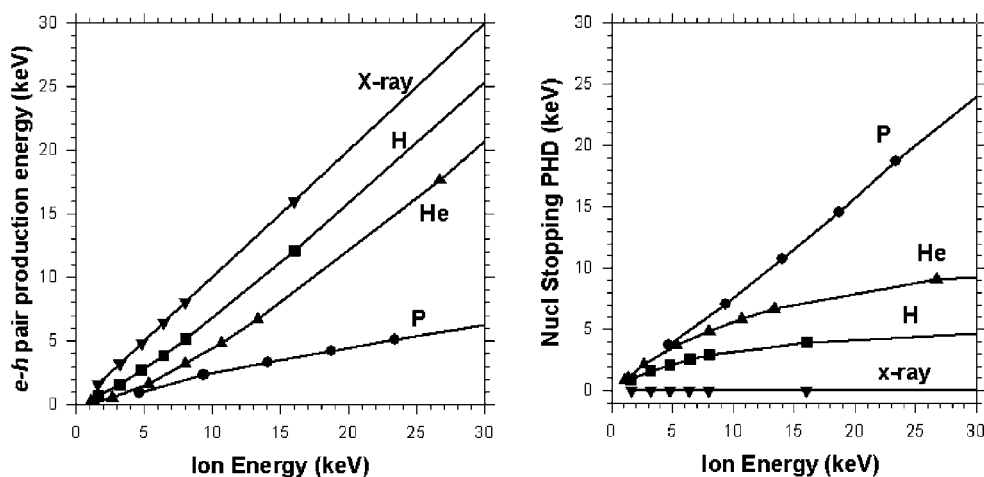


Fig. 2. Comparison of the pulse-height-defect (PHD) values between different incident ions and X-rays.

based on the work by Haines and Whitehead.¹⁰⁾ Due to the PHD problem, the detection of keV P^+ ions, required for implantation of shallow donors, is a highly challenging task. To our knowledge, no work has been reported in literature on the detection of single heavy ions, such as P^+ , at sub-50 keV by semiconductor detectors.

As an example of the challenge, consider a P^+ ion with an initial energy of 15 keV. The ion loses about 4 keV after passing through a 7 nm SiO_2 dead-layer and arrives in the active silicon substrate with 11 keV incident energy. There it contributes only 2 keV to ionization energy resulting in the production of $(2000 \text{ eV})/(3.6 \text{ eV/e-h pair}) \sim 560$ e-h pairs. Here 3.6 eV is the energy required to create one e-h pair in silicon. The detector has to be constructed in a way to maximize the charge collection efficiency, so that a signal with a significant pulse height can be produced.

In Fig. 3, a technology computer aided design (TCAD) simulation of a single ion impact indicates a rapid charge sweeping across the area between 8 V biased electrodes. On the actual device, these were made of aluminum by a vacuum-vapor-deposition process, on the top of a 5 nm SiO_2 layer grown on the top of a pure silicon wafer ($>5000 \Omega\text{cm}$). With a $20 \mu\text{m}$ separation between the two electrodes, the positively biased electrode is coupled to the input JFET of a charge sensor, which is constructed to be operated in a charge-sensitive-amplification mode. Use of a charge sensitive preamplifier gives maximum sensitivity in the detection of the induced charge, and has the advantage that the charge pulse height is linearly proportional to the number of e-h pairs produced.

The principle of the charge pulse formation in the ion detector is the same as that in the standard radiation detectors, such as a Si(Li) detector for X-rays or a double-sided strip-detector for high-energy GeV particles. The generation of an induced current in the sensor electrodes is governed by the Ramo-Shockley theorem.^{11,12)} The induced current rises immediately when the e-h carriers start to drift under the influence of an electric field introduced by an electrical bias between the paired-electrodes, and ends when

the electron and hole carriers arrive in the separated electrodes. TCAD simulation reveals that the drifting process can be completed within a few nanoseconds.¹³⁾ The charge pulse is formed by integration of the induced current and direct current in the signal electrode coupled to a charge-sensitive-amplifier with a typical integration time of about 1 μs . Note that the complete integration of the induced current yields an amount of charge equal to the charge of one type of carrier generated by the ionization energy involved. In the sensor capacitor (feedback capacitor), the accumulated charge is contributed by the induced charge from the drifting charge carriers and from the DC leakage current. The accumulated charge will slowly discharge completely in a period of between 1 ms and 200 ms, depending on the type of the feedback network employed in the system.

4. Characterization of keV Ion Detectors

The detector for the keV P^+ ion implantation detection has to be constructed in a way to be compatible with the subsequent device fabrication processes. The detector electrodes have to be set sufficiently apart to accommodate the components of the device. To measure the charge collection efficiency as a function of electrode spacing, we use focused 2 MeV helium ions in a nuclear microprobe to map the charge collection efficiency in a prototype detector through the standard IBIC method.¹⁴⁾ Figure 4 displays the layout of the detector coupled with the supporting electronics and the experimental results of the charge collection efficiency measurement. 2 MeV helium ions have a negligible PHD effect and the full energy can be assumed to contribute to ionization energy producing a large number of e-h pairs: $(2 \times 10^6 \text{ eV})/(3.6 \text{ eV/e-h pair}) \sim 5.6 \times 10^5$ e-h pairs. The charge pulse of 2 MeV helium ions is 3 orders of magnitude higher than that of 15 keV P^+ ions, therefore standard instrumentation can be used to carry out the measurements at 300 K. The results show that nearly 100% efficiency has been achieved in this prototype detector developed for the 15 keV P^+ ion implantation and detection.

The IBIC measurement can also provide information on the thickness of the inactive layer (dead-layer), which takes up a small part of ion energy without producing any detectable e-h pairs. The dead-layer thickness can be deduced by the measurement of the reduction in charge pulse height with increasing ion incident angle in the substrate. A typical dead-layer thickness, equivalent to 5–7 nm SiO_2 , was measured from the IBIC experiment.¹⁵⁾

5. Online Detection of Single sub-20 keV P^+ Ion Implantation Events

When 15 keV P^+ ions are implanted into silicon, only a small proportion ($2 \text{ keV}/15 \text{ keV} \sim 13\%$) of the energy produces ionization yielding about 560 e-h pairs as previously stated. In order to detect such low-energy P^+ impacts with a high signal-to-noise ratio, it is essential to employ a low noise charge-sensitive preamplifier. The charge-sensitive preamplifier typically contains a JFET for coupling to the detector itself and a feedback capacitor C_f , for converting accumulated charge into a voltage pulse $V_{\text{out}} \sim Q/C_f$, as shown in Fig. 5. C_f is typically as small as possible, normally about 10 fF (for keV ions) to 1 pF (for MeV ions), depending on the number of e-h pairs (ionization

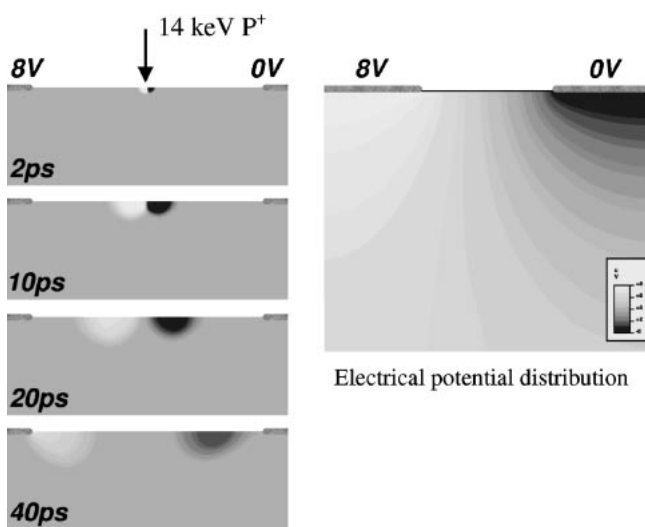


Fig. 3. Technology Computer Aided Design (TCAD) simulation of a single ion impact indicates a rapid charge sweeping across the area between 8 V biased electrodes.

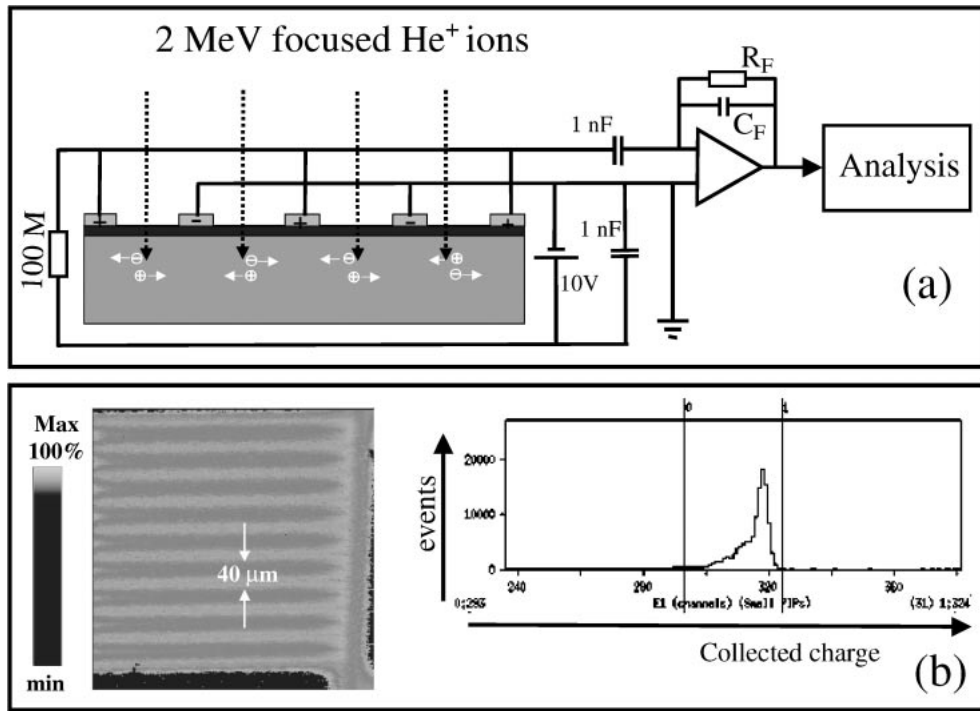


Fig. 4. (a) Layout of the detector coupled with the supporting electronics; (b) experimental results of the charge collection efficiency measurement. Nearly 100% efficiency has been achieved in this prototype detector developed for the 15 keV P⁺ ion implantation and detection. 2 MeV He⁺ ions and standard instruments are used to carry out the measurement at 300 K temperature.

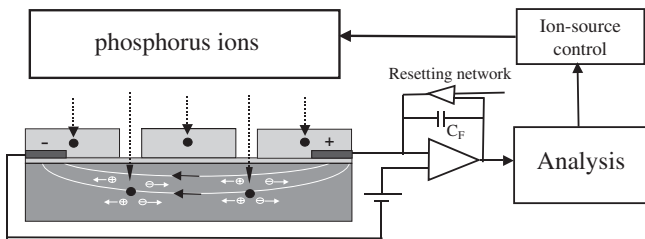


Fig. 5. Layout of the on-demand-control operation of single ion implantation. The PMMA nanometer mask on the top of the detector is for the accurate positioning of the single ion implantation site. The detector signal is fed to control the ion source.

energy) per incident ion.

The overall noise of the detection system comes from two sources: detector electronic noise and detector intrinsic noise. The noise level of the current keV ion detection system is dominated by the detector electronic noise, with a major contribution from the detector leakage current ($i_{\text{noise}}^2 = 2eI_{\text{DET}}$, where the I_{DET} is a detector leakage current, about 50 pA at 3 V bias across the paired electrodes with 20 μm spacing at room temperature. The detector intrinsic noise is due to the statistical fluctuation of the number of e-h pairs produced by the ionization energy dissipation in the system.

For example, the $N_{\text{e-h}} = 560$ e-h pairs created from a single 15 keV P⁺ ion have a standard variance: $\delta N = (FN_{\text{e-h}})^{1/2} = 8.2$ e-h pair, where F is the Fano factor 0.12. The statistical variation is $\delta N_{\text{e-h}}/N_{\text{e-h}} \sim 1.5\%$, which is much smaller than the minimum achievable electronic energy resolution, typically about 0.2 keV/2 keV $\sim 10\%$ for the

measurement of 2 keV ionization energy. Therefore, the electronic noise dominates the ultimate energy resolution in the keV ion detection system and hence dominates the FWHM of the experimental pulse height spectrum, shown in Fig. 6 for 14 keV P⁺ ions.

6. Fabrication of Two Qubits System

The single ion detection system has been integrated into the fabrication process for the construction of two qubit devices.^{16,17} Figure 7(a) illustrates the integration of key components: two electrodes of 10 μm spacing were aluminum-vapor-deposited on a 5 nm SiO₂ layer on the surface of a pure silicon wafer which was then spin-coated with 70 nm PMMA and subsequently fabricated with two apertures with 30 nm diameter and 60 nm spacing by e-beam lithography. The aperture sites can be relocated later with the assistance of metal alignment markers fabricated on the silicon wafer with e-beam lithography.

After implantation and registration of two P⁺ ions in the detection system, with a 50% chance each aperture site received one P⁺ ion and a 50% chance 2 ions passed through the same aperture, the subsequent process was to lift off the PMMA layer and fabricate qubits gates, and the read-out system, which consists of two sets of single electron transistors (SET), as shown in Fig. 7(b).

7. Conclusions

We developed a single ion implantation and online detection method, to be compatible with the nano fabrication process required for the fabrication of structures for a quantum computer. The method was integrated into the construction pathway for a prototype two donor device.

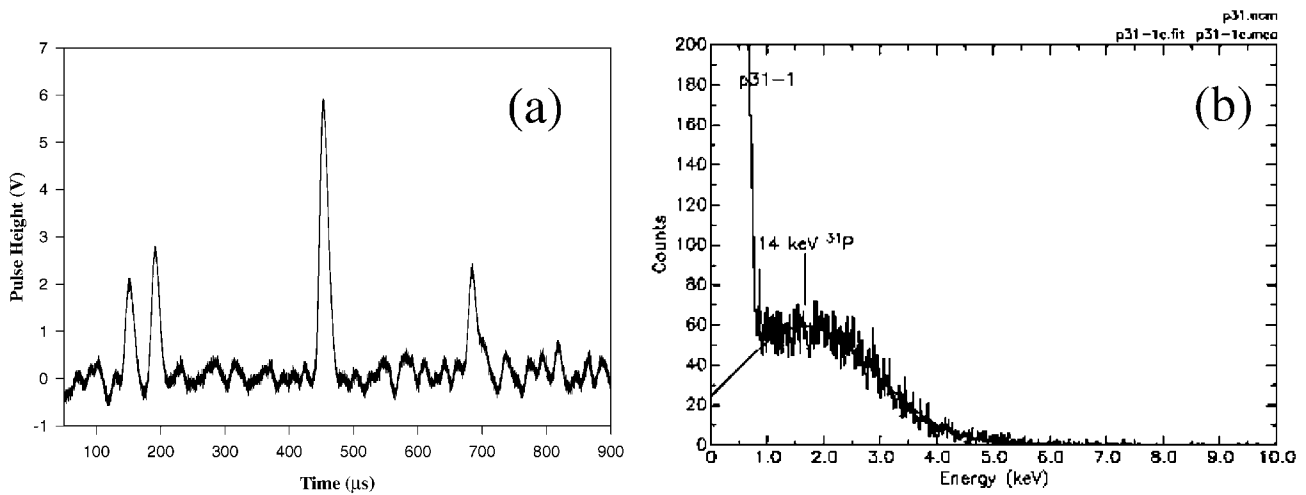


Fig. 6. Results of 14 keV P^+ ions detection in a prototype of testing devices. (a) Charge pulses corresponding to single P^+ ion impacts; (b) charge pulse height spectrum of the ion induced charge pulses.

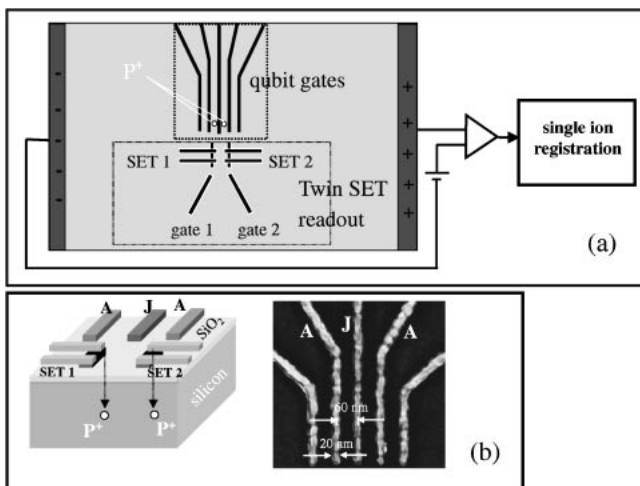


Fig. 7. (a) The single ion detection system has been integrated into the fabrication process for the construction of two qubit devices. (b) Nanofabrication steps for the qubit gates and readout SETs.

Acknowledgements

We acknowledge the financial supports provided by Australian Research Council under the Special Research Centre Scheme and by the US Government under ARO grant DAAA 19-01-1-0563.

- 1) B. E. Kane: *Nature* **393** (1998) 133.
- 2) J. L. O'Brien, S. R. Schofield, M. Y. Simmons, R. G. Clark, A. S. Dzurak, N. J. Curson, N. S. McAlpine, M. E. Hawley and G. W.

- Brown: *Phys. Rev. B* **64** (2001) 161401.
- 3) D. N. Jamieson: *Proc. First Int. Conf. Quantum Computers*, January 16–19, 2001, Sydney, Australia.
- 4) C. Yang, B. L. Doyle, P. Rossi, M. Nigam, M. El Bouanani, J. L. Duggan and F. D. McDaniel: *Nucl. Instrum. & Methods Phys. Res. B* **191** (2001) 329.
- 5) T. Shinada, A. Ishikawa, C. Hinoshita, M. Koh and I. Ohdomari: *Jpn. J. Appl. Phys.* **39** (2000) L265.
- 6) T. Shinada, A. Ishikawa, M. Fujita, K. Yamashita and I. Ohdomari: *Jpn. J. Appl. Phys.* **38** (1999) 3419.
- 7) T. Schenkel, J. Meijer, A. Persaud, J. W. McDonald, J. P. Holder and D. H. Schneider: *Proc. SPIE* **4656**, *Int. Symp. Integrated Optoelectronic Devices, Nanotechnology in Photonics-Quantum computing and Information*, San Jose, CA, January 2002.
- 8) D. McCammon *et al.*: *Nucl. Instrum. & Methods Phys. Res. A* **326** (1993) 157.
- 9) J. Lindhard, M. Scharff and H. E. Schiott: *Medd. Dan. Vid. Selsk.* **33** (1963) 14.
- 10) E. L. Haines and A. B. Whitehead: *Rev. Sci. Instrum.* **37** (1966) 190.
- 11) S. Ramo: *Proc. IRE* **27** (1939) 584.
- 12) W. Shockley: *J. Appl. Phys.* **9** (1938) 635.
- 13) C. I. Pakes, D. P. George, D. N. Jamieson, C. Yang, A. S. Dzurak, E. Gauja and R. G. Clark: *Nanotechnology* **14** (2003) 161.
- 14) M. B. H. Breese, D. N. Jamieson and P. J. C. King: *Material Analysis Using a Nuclear Microprobe* (John Wiley & Sons, Inc, 1996).
- 15) C. Yang, D. N. Jamieson, S. M. Hearne, C. I. Pakes, B. Rout, E. Gauja, A. J. Dzurak and R. G. Clark: *Nucl. Instrum. & Methods Phys. Res. B* **190** (2002) 212.
- 16) F. E. Stanley, T. M. Buehler, R. P. McKinnon, E. Gauja, K. Peceros, L. D. Macks, V. Chan, M. Mitic, A. S. Dzurak, R. G. Clark, C. I. Pakes, C. Yang, D. N. Jamieson and S. Praver: to be published in *ICPS Proc.* 2002.
- 17) D. N. Jamieson, C. Yang, C. I. Pakes, S. M. Hearne, S. Praver, A. S. Dzurak and R. G. Clark: *17th Int. Conf. Application of Accelerators in Research and Industry-CAARI-2002* November 12–16, 2002, Texas, USA.